Proc. Natl. Acad. Sci. USA
Vol. 80, pp. 4325–4329, July 1983
Biophysics

New view of lipid bilayer dynamics from ^2H and ^{13}C NMR relaxation time measurements*

(frequency dependence/order fluctuations/vesicles/microviscosity/liquid crystals)

MICHAEL F. BROWN†, ANTHONY A. RIBEIRO‡, AND GERALD D. WILLIAMS†

†Department of Chemistry, University of Virginia, Charlottesville, Virginia 22901; and ‡Stanford Magnetic Resonance Laboratory, Stanford University, Stanford, California 94305

Communicated by Harden M. McConnell, April 7, 1983

ABSTRACT **Natural abundance ^{13}C spin-lattice (T_1) relaxation time measurements are reported for unilamellar vesicles of 1,2-dipalmitoylphosphatidylcholine (1,2-dipalmitoyl-*sn*-glycero-3-phosphocholine), in the liquid crystalline phase, at magnetic field strengths of 1.40, 1.87, 2.35, 4.23, 7.05, 8.45, and 11.7 tesla (resonance frequencies of 15.0, 20.0, 25.1, 45.3, 75.5, 90.5, and 126 MHz, respectively), and the results are compared to previous ^2H T_1 studies of multilamellar dispersions. For both the ^{13}C and ^2H T_1 studies, a dramatic frequency dependence of the relaxation was observed. At superconducting magnetic field strengths (4.23–11.7 tesla), plots of the ^{13}C T_1^{-1} relaxation rates as a function of acyl chain segment position clearly reveal the characteristic "plateau" signature of the liquid crystalline phase, as found previously from ^2H NMR studies. The dependence of T_1^{-1} on ordering, determined previously from ^2H NMR, and the T_1^{-1} dependence on frequency, determined from both ^{13}C and ^2H NMR studies, suggest that a unified picture of the bilayer molecular dynamics can be provided by a simple relaxation law of the form $T_1^{-1} \approx A\tau_f + BS_{C\text{-}H}^2 \omega_0^{-1/2}$. In the above expression, *A* and *B* are constants, $S_{C\text{-}H}$ ($=S_{C\text{-}D}$) is the bond segmental order parameter, and ω_0 is the nuclear Larmor frequency. The first (*A*) term includes contributions from fast, local segmental motions characterized by the effective correlation time τ_f, whereas the second (*B*) term describes slower, collective fluctuations in the local ordering. The value of $\tau_f \approx 10^{-11}$ sec, obtained by extrapolating T_1^{-1} to infinite frequency, suggests that the segmental microviscosity of the bilayer hydrocarbon region does not differ appreciably from that of the equivalent *n*-paraffinic liquids of similar chain length.**

NMR techniques were among the first biophysical methods to be applied to lipid bilayers and biological membranes (1, 2). Perhaps the foremost progress in recent years has been made in applications of NMR lineshape analysis to studies of the molecular ordering and conformations of membranous lipids (3–7). Yet, in spite of early promise (8–11), the interpretation of nuclear spin relaxation experiments has not progressed similarly and, in fact, has remained an outstanding problem in membrane biophysics for more than a decade (cf. ref. 12). The bulk of previous work has involved spin-lattice (T_1) relaxation time measurements, which are sensitive to details of the molecular motions in the MHz region. Perhaps the major justification for T_1 relaxation studies of membranes is their dual character as both solid-like and liquid-like materials. The analogies to simpler liquid crystals point to the necessity of obtaining both *static* and *dynamic* information in defining these systems and of distinguishing membranes from other classes of biological macromolecules, such as the globular and fibrous proteins and the nucleic acids. These latter biopolymers, while also rich in dynamic behavior (13, 14), appear to have fairly well-defined average structures that can be directly related to their biological function. No analogous relationships between membrane structure and function are known to exist at present, although some general properties have emerged from biophysical studies (4, 6, 7, 15–18).

Thus, in seeking to further delineate possible structure–function relationships in biomembranes, their characteristics as biological liquid crystals may merit further detailed consideration. Because high-resolution diffraction techniques are generally restricted to crystalline materials, NMR can be expected to play an increasingly important role in the elucidation of membrane physical properties. The interpretation of NMR relaxation times in terms of lipid bilayer dynamics ultimately rests on the introduction of specific motional models, which must lead to experimentally testable predictions before their physical significance can be evaluated. Most recent literature discussions have tended to focus on one or more of the following paradigms: (*i*) simple isotropic or anisotropic diffusion models (9, 10) modified to include ordering effects (19–21), (*ii*) multiple internal rotation models for acyl chain dynamics (22–24), and (*iii*) simplified two-motion models in which the fast component is as in (*i*) and the slow component is identified either with "rigid body motions" (25, 26) or with collective bilayer disturbances (12, 27, 28).

Until very recently, the lack of sufficiently detailed T_1 data has severely limited our ability to distinguish among the various competing theoretical models. The interpretation of ^1H NMR results (9, 25, 26) is complicated by possible spin diffusion, together with uncertainties in separating intra- from intermolecular effects, making quantitative analysis difficult. Studies with ^2H and ^{13}C NMR avoid these difficulties, and ^2H NMR, particularly, is widely viewed as a promising technique because information on both molecular dynamics and ordering can be obtained (19). Natural abundance ^{13}C NMR is a useful adjunct to ^2H NMR in that (*i*) isotopic labeling is unnecessary, thereby allowing studies of a wide range of lipid bilayers and biological membranes (29, 30), and (*ii*) the relaxation is sensitive to higher frequency motions than in ^2H NMR because T_1 depends on both the ^{13}C and ^1H Larmor frequencies. Moreover, high-resolution ^{13}C NMR spectra can now be obtained, and relaxation studies can be performed at natural abundance for either multilamellar lipid dispersions with cross-polarization/magic-angle spinning (7, 31) or unilamellar vesicles with conventional Fourier transform techniques. For ^{13}C T_1 studies, the use of vesicles is presently attractive because little change in T_1 is observed with sonication (19, 31), and one can directly measure the frequency

The publication costs of this article were defrayed in part by page charge payment. This article must therefore be hereby marked "*advertisement*" in accordance with 18 U.S.C. §1734 solely to indicate this fact.

Abbreviation: Pam_2-PtdCho, 1,2-dipalmitoylphosphatidylcholine (1,2-dipalmitoyl-*sn*-glycero-3-phosphocholine).

* Based on a talk presented at 10th International Conference on Magnetic Resonance in Biological Systems, Stanford University, August, 1982.

dependence of T_1 by using conventional NMR systems operating at different fixed magnetic field strengths. The present paper (*i*) summarizes the results of ^2H T_1 studies of multilamellar dispersions of 1,2-dipalmitoylphosphatidylcholine (Pam_2-PtdCho; 1,2-dipalmitoyl-*sn*-glycero-3-phosphocholine) and (*ii*) describes recent ^{13}C T_1 studies of vesicles of Pam_2-PtdCho at *seven* different magnetic field strengths (i.e., resonance frequencies). Previous ^{13}C T_1 studies of Pam_2-PtdCho vesicles have been limited to *one* magnetic field strength (8, 11, 22, 23). Both the ^2H and the ^{13}C T_1 data can be explained best in terms of a dominant contribution to the acyl chain relaxation from collective bilayer modes, as described below.

RESULTS AND DISCUSSION

A summary of previous ^2H NMR studies of specifically deuterated Pam_2-PtdCho multilamellar dispersions in the liquid crystalline (L_α) phase (12, 19, 32) is provided in Fig. 1. The observed ^2H spin-lattice relaxation rates, T_1^{-1}, of the C-4, C-8, and C-14 acyl chain segments depend on the nuclear resonance frequency—i.e., the magnetic field strength at which the measurements are performed. Both (*i*) the magnitude of the ^2H T_1 values and (*ii*) their observed increase with temperature are inconsistent with a single type of fast diffusive motion as the source of the frequency dependence—even if extremes of diffusion tensor anisotropy and ordering are assumed (12). Rather, the data are best explained in terms of contributions to T_1 from different motional components with distinctive amplitudes and time scales.

In the following presentation, it is assumed that the observed T_1^{-1} relaxation rate is the sum of two independent contributions, as indicated below

$$1/T_1 = 1/T_{1f} + 1/T_{1s}, \qquad [1]$$

where T_{1f}^{-1} indicates the contribution from relatively fast motions, and T_{1s}^{-1} is the contribution from slower motions. For reasons discussed in further detail elsewhere (12), the ^2H T_1^{-1} data are plotted in Fig. 1 both vs. $\omega_D^{-1/2}$ (Fig. 1*a*) and vs. ω_D^{-2} (Fig. 1*b*), where ω_D is the ^2H resonance frequency (rad s^{-1}). The $\omega_D^{-1/2}$ dependence is characteristic of a collective model for relatively slow motions in the liquid crystalline phase (12, 27) in which the orientational fluctuations of the lipid moieties are described in terms of a continuous distribution of wave-like disturbances. The ω_D^{-2} dependence, on the other hand, would describe slow motions of a somewhat less collective nature, assuming that the frequency cutoff $1/\tau_s$ falls into the long correlation time regime. Those motions that might lead to a ω_D^{-2} dependence could include relatively uncorrelated "rigid body motions" of phospholipids in the bilayer (25, 26) and relatively slow rotational diffusion of phospholipids or their acyl chains about the bilayer normal, if the quadrupolar interaction is not cylindrically averaged over a faster time scale.

Because ^2H T_1 data are available at only three magnetic field strengths, i.e. resonance frequencies, it is not possible to distinguish among the various motional models based *solely* on the observed frequency dependence (12). However, the dependence on ordering is most typical of a collective-type model and disfavors an interpretation in terms of noncollective "rigid body motions" (25, 26) or phospholipid rotational diffusion. For, as shown in Fig. 1*a Inset*, T_1^{-1} is observed to depend on the square of the ^2H order parameter, $S_{C\text{-}D}$, for all acyl chain segment positions of the bilayer at all temperatures (12). The observation that $T_1^{-1} \propto S_{C\text{-}D}^2$ is consistent with the presence, in the liquid crystalline phase of lipid bilayers, of fast effective motions, which project the residual quadrupolar interaction onto a local or instantaneous symmetry axis. These fast, axially symmetric motions would then dominate any contributions from slower phospholipid rotational diffusion to T_1^{-1} (convolution theorem). Although both the collective- and noncollective-type slow motional models can predict the observed dependence of T_1^{-1} on $S_{C\text{-}D}^2$ for reasons discussed elsewhere (12), only the collective model is in quantitative agreement with the results. Thus, the data summarized in Fig. 1*a* are most consistent with a relaxation law of the form (12)

$$1/T_1 \cong A\tau_f + BS_{C\text{-}H}^2\omega_0^{-1/2}, \qquad [2]$$

where $T_1^{-1} \equiv T_{1f}^{-1} + T_{1s}^{-1}$ (i.e., the fast and slow motional contributions to the relaxation rate are additive, and cross-correlations are ignored to a first approximation). In Eq. 2, $S_{C\text{-}H}$ (= $S_{C\text{-}D}$) is the bond segmental order parameter, ω_0 is the resonance frequency, and A and B are constants that depend on the particular nucleus of interest.

At present, little can be said regarding the relative amplitudes of the suggested fast and slow motional components. However, the observations of (*i*) a T_1^{-1} frequency dependence together with (*ii*) a "plateau" in both the T_1^{-1} and ordering profiles as a function of chain position (4, 6, 18, 19) are very important and suggest a connection between the *ordering* and *dynamics* of the Pam_2-PtdCho bilayer as assessed from NMR

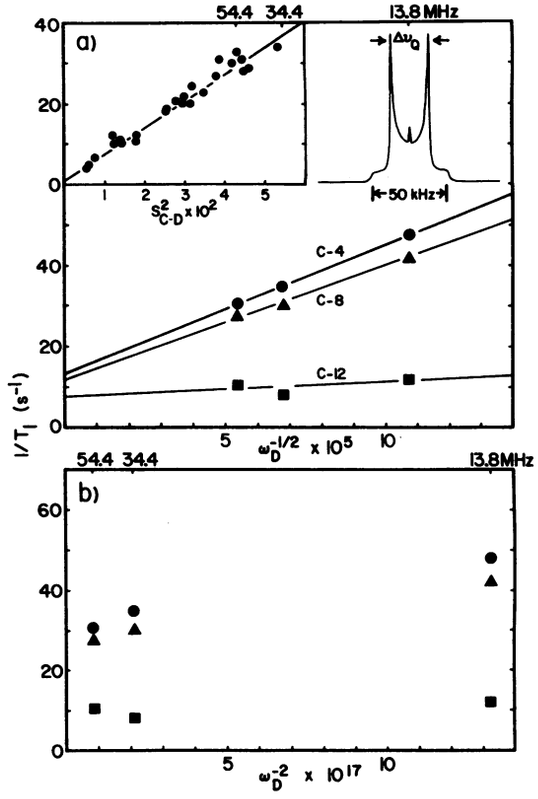

FIG. 1. Summary of ^2H spin-lattice relaxation time T_1 measurements of specifically deuterated Pam_2-PtdCho multilamellar dispersions, containing 50% (wt/wt) H_2O in the liquid crystalline phase at 51°C. The studies were performed at resonance frequencies of 13.8, 34.4, and 54.4 MHz (magnetic field strengths of 2.11, 5.26, and 8.32 tesla, respectively) (19, 32). (*a*) Plot of the ^2H spin-lattice relaxation rate T_1^{-1} of the C-4 (●), C-8 (▲), and C-12 (■) acyl chain segments vs. $\omega_D^{-1/2}$, where ω_D is the ^2H resonance frequency. (*Left Inset*) ^2H T_1^{-1} values obtained at 54.4 MHz plotted vs. the ^2H order parameter $S_{C\text{-}D}^2$ for all acyl chain segment positions at all temperatures for which data are available (12). The segmental order parameter $S_{C\text{-}D}$ is related to the residual quadrupolar splitting $\Delta\nu_Q$ of the powder-type ^2H NMR spectra (*Right Inset*) by the relationship $S_{C\text{-}D} = [3/4(e^2qQ/h)]^{-1}\Delta\nu_Q$, where (e^2qQ/h) = 170 kHz for aliphatic C—^2H bonds (4). (*b*) Plot of the same ^2H T_1^{-1} values for the C-4, C-8, and C-12 chain segments vs. ω_D^{-2}.

studies. Physically, the first term of Eq. 2 would correspond to fast or local effective motions of the lipid acyl chain segments (e.g., due to *trans–gauche*$^{\pm}$ isomerizations, torsions, etc.) with respect to a local director axis of approximately cylindrical symmetry. The second term describes cooperative fluctuations of this instantaneous director axis with regards to the macroscopic bilayer normal (average director). Thus, the local ordering set up by the rapid acyl chain fluctuations could be modulated by any collective motions of larger amplitude (e.g., corresponding to wave-like disturbances in the bilayer as mentioned above), which for simplicity are modeled here by using a continuum description (33). The collective bilayer modes, each with a characteristic amplitude and correlation time, would undergo highly damped or viscous first-order relaxation, leading in a continuum description to the postulated $\omega_D^{-1/2}$ dependence in the frequency domain.

What further experimental findings exist in support of the above interpretation? Recently, we have performed ^{13}C T_1 studies of Pam_2-PtdCho unilamellar vesicle suspensions as a function of frequency (30), which complement the ^2H NMR studies of specifically deuterated Pam_2-PtdCho multilamellar dispersions. Such natural abundance ^{13}C NMR studies are useful in view of the different range of resonance frequencies relative to ^2H NMR, so that one can obtain a more complete picture of the bilayer dynamics than is possible with either technique alone. Fig. 2*a* shows a summary of profiles of the ^{13}C T_1^{-1} relaxation rates vs. acyl chain segment position, obtained for Pam_2-PtdCho vesicles in the liquid crystalline phase, at *seven* different magnetic field strengths (i.e., resonance frequencies). Qualitatively, it can be seen from Fig. 2*a* that T_1 increases rather substantially with increasing magnetic field strength (T_1^{-1} decreases) as observed from ^2H NMR studies (Fig. 1). For the case of ^{13}C NMR, T_1^{-1} varies by more than a factor of 2 over the range of resonance frequencies investigated. With the increased resolution at the higher magnetic field strengths (4.23–11.7 tesla), the main acyl chain methylene envelope, corresponding to carbons C-4 to C-13, is clearly seen to be non-Lorentzian and further splits up into three or more resolved components (see, for instance, the spectrum in Fig. 2*a*). This observation is of key importance, for it can be shown that the ^{13}C T_1^{-1} relaxation rates, within experimental error, vary only slightly across the inhomogeneously broadened methylene envelope from C-4 to C-13 (i.e., a "plateau" in the ^{13}C T_1^{-1} rates vs. acyl chain position exists as indicated by the dotted lines in Fig. 2*a*). (The above observations do not preclude relatively small variations in the ^{13}C T_1^{-1} rates among the unresolved CH_2 groups, so that the squared-off edges of the ^{13}C T_1^{-1} profiles may be somewhat misleading for the longer chain saturated phospholipids such as Pam_2-PtdCho).

For comparison, Fig. 2*b* shows the available ^2H T_1^{-1} profiles vs. chain segment position for specifically deuterated Pam_2-PtdCho multilamellar dispersions at the three resonance frequencies (19, 32) and shows plots of the ^2H order parameter $S_{C\text{-}D}$ vs. acyl chain segment position determined at 54.4 MHz (19). Qualitatively, both the ^2H T_1^{-1} and $S_{C\text{-}D}$ values show a "plateau" when plotted as a function of acyl chain segment position (4, 6, 18, 19). In addition, ^2H T_1^{-1} values are included in Fig. 2*b* for unilamellar vesicles of Pam_2-PtdCho selectively deuterated at the C-4 segment at 13.8 MHz (unpublished data) and for the C-2, C-4, and C-14 positions at 54.4 MHz (19), evincing that only minimal changes in T_1^{-1} occur upon sonication. The latter observations are consistent with recent natural abundance ^{13}C T_1^{-1} studies that use cross-polarization/magic-angle spinning techniques (31). The obvious qualitative similarity of the ^{13}C T_1^{-1} profiles obtained over a wider frequency range to the more limited ^2H T_1^{-1} profiles clearly supports pre-

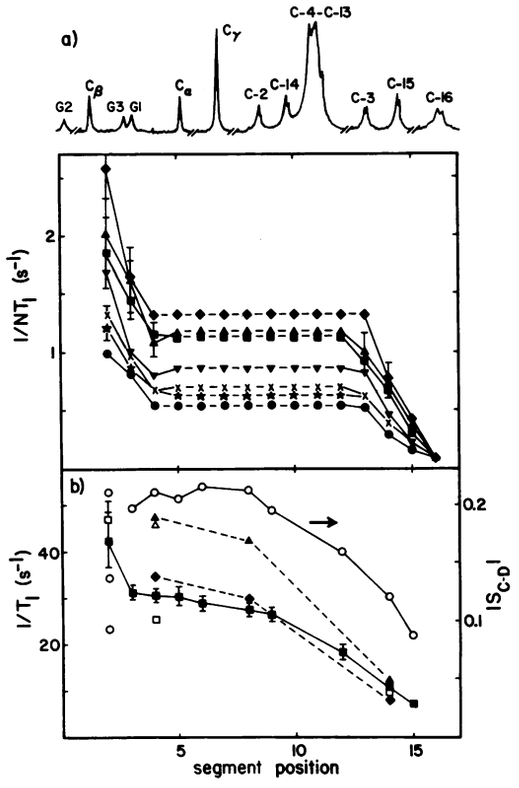

FIG. 2. ^{13}C and ^2H spin-lattice relaxation rate profiles obtained for the Pam_2-PtdCho bilayer at 50–51°C as a function of magnetic field strength, i.e. resonance frequency. (*a*) Representative, natural abundance ^{13}C NMR spectrum of unilamellar Pam_2-PtdCho vesicles at 50°C and 126 MHz (11.7 tesla), together with resonance assignments (8, 11) and plots of $(NT_1)^{-1}$ vs. chain position, where N is the number of directly bonded protons. Note particularly the non-Lorenztian shape of the acyl chain envelope profile from C-4 to C-13, which is resolved into three or more components at the higher magnetic field strengths (7.05–11.7 tesla), and the well-resolved doublets from those carbons near the chain ends, which are due either to chain inequivalence (4, 6) or to chemical shift differences between the two monolayers of the unilamellar vesicles. The acyl chain carbons are designated C-1 through C-16; the three glycerol carbons are G1–G3 (stereospecific numbering); and the three head group segments are C_α, C_β, and C_γ, where C_α indicates the position closest to the phosphodiester moiety (6). The data refer to the following resonance frequencies (magnetic field strengths) and were obtained at the indicated NMR facilities: ◆, 15.0 MHz (1.40 tesla), University of Virginia, JEOL FX-60Q spectrometer; ▲, 20.0 MHz (1.87 tesla), State University of New York, Stony Brook, Varian CFT-20 spectrometer; ■, 25.1 MHz (2.35 tesla), University of Virginia, JEOL PFT-100 spectrometer; ▼, 45.3 MHz (4.23 tesla), University of California, Berkeley, using home-built system; ×, 75.5 MHz (7.05 tesla), State University of New York, Stony Brook, Nicolet NT-300 spectrometer; ★, 90.5 MHz (8.45 tesla), University of Virginia and Stanford Magnetic Resonance Laboratory, Nicolet NT-360 and Bruker HXS-360 spectrometers, respectively; and ●, 126 MHz (11.7 tesla), National Institutes of Health, Nicolet NT-500 spectrometer system. In all cases, the T_1 relaxation times were measured by the inversion recovery (180°–τ–90°) pulse method (34). Solid lines connect those symbols corresponding to single carbon resonances or to the average $(NT_1)^{-1}$ values for those cases where doublets are observed. Dashed lines connect those symbols corresponding to the average relaxation rate of the methylene envelope carbons. The high- and low-frequency shoulders of the CH_2 envelope are tentatively ascribed to the C-4 and C-13 carbons, respectively. (*b*) Summary of previously obtained ^2H T_1^{-1} relaxation rate and order profiles for specifically deuterated Pam_2-PtdCho multilamellar dispersions as a function of acyl chain segment position at 51°C (19, 32). ▲, T_1^{-1} at 13.8 MHz (2.11 tesla); △, corresponding T_1^{-1} value for C-4 of sonicated vesicles at 13.8 MHz; ◆, T_1^{-1} at 34.4 MHz (5.26 tesla); ■, T_1^{-1} at 54.4 MHz (8.32 tesla); □, corresponding T_1^{-1} values for vesicles at 54.4 MHz; ○, the ^2H order parameter $S_{C\text{-}D}$ measured at 54.4 MHz.

sentation of the data as indicated in Fig. 2*a*.

The more comprehensive ^{13}C T_1 relaxation time data as a function of frequency can be analyzed in terms of models for the molecular dynamics of lipid bilayers in a manner analogous to that for ^2H NMR (12). Fig. 3 shows the ^{13}C T_1^{-1} values of the bulk acyl chain methylene groups of the Pam_2-PtdCho vesicles [i.e., representing those CH_2 groups in the "plateau" region of the acyl chains (Fig. 2*a*)] plotted vs. $\omega_C^{-1/2}$ (Fig. 3*a*) and vs. ω_C^{-2} (Fig. 3*b*), where ω_C is the ^{13}C nuclear resonance frequency. For the case of ^{13}C NMR, the increased number of data points relative to ^2H NMR (see Fig. 1) clearly allows a distinction to be made among the various models for slow motions. The ^{13}C NMR data yield straight lines when T_1^{-1} is plotted vs. $\omega_C^{-1/2}$ (Fig. 3*a*), whereas if T_1^{-1} is plotted vs. ω_C^{-2} (Fig. 3*b*), curved lines result. Thus, models which predict that $T_1^{-1} \propto \omega_C^{-2}$ [e.g., a "rigid body motion" model of the type suggested by Chan and coworkers (25, 26)] can be ruled out with some confidence at present, and Pace and Chan (28) now appear to agree with our interpretation.

Could relatively slow phospholipid rotational diffusion about the bilayer normally account for the ^{13}C T_1^{-1} frequency dependence in the liquid crystalline phase? Putting aside the previous symmetry arguments from ^2H NMR for the moment (*vide supra*), if a contribution from phospholipid or acyl chain rotation with $\tau_s \approx 10^{-8}$ sec were to strongly influence the frequency dependence of T_1, then we should be able to observe a T_1 minimum (35) under certain conditions. The fact that the T_1 relaxation times of the Pam_2-PtdCho bilayer acyl chain segments increase with temperature for all nuclei (^1H, ^2H, and ^{13}C) at all frequencies investigated (8–11, 19, 22, 26, 30, 32) makes it implausible that we are near such a T_1 minimum; thus, it again can be concluded that a significant contribution from phospholipid or fatty acyl chain rotational diffusion to the T_1 frequency dependence is unlikely.

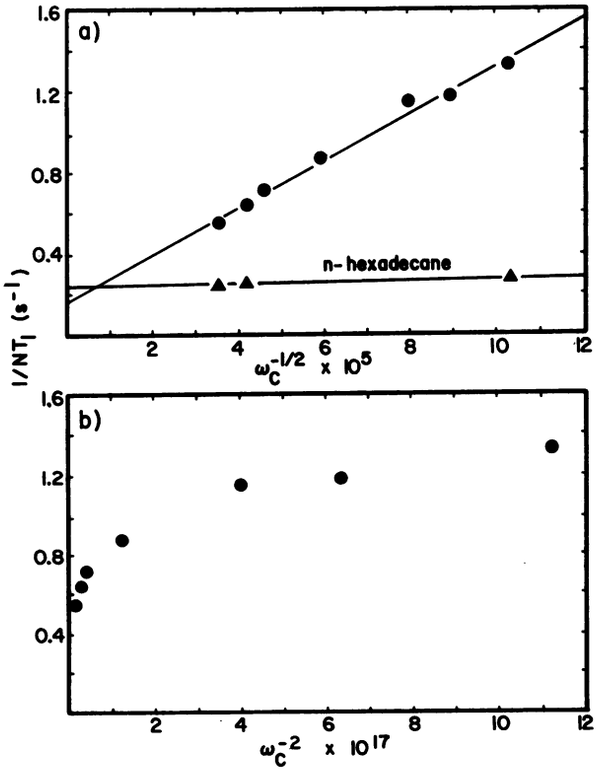

FIG. 3. Plots of ^{13}C $(NT_1)^{-1}$ values obtained for the C-4-to-C-13 acyl chain carbon envelope of the Pam_2-PtdCho vesicles at 50°C (cf. Fig. 2*a*) vs. $\omega_C^{-1/2}$ (*a*) and ω_C^{-2} (*b*).

Both the ^2H and ^{13}C NMR relaxation rates of the Pam_2-PtdCho bilayer hydrocarbon region would then appear best explained by a law of the form of Eq. 2 in which the first term describes local diffusive motions (19, 20), and the dependence of T_1^{-1} on frequency and ordering is rationalized by a second contribution from collective bilayer fluctuations (12). Preliminary studies of a homologous series of 1,2-diacylphosphatidylcholines with fatty acyl chains ranging in length from laurate (12:0) to stearate (18:0) suggest that Eq. 2 describes the ^{13}C T_1 relaxation of these systems as well, in the liquid crystalline phase (30). Assuming that the T_{1f}^{-1} term as given by the intercepts of Fig. 1*a* or Fig. 3*a* is small relative to the T_{1s}^{-1} term, the temperature dependence of T_1^{-1} could then be governed by the slow motional contribution (12, 30). This suggestion is supported by the observation that $T_1^{-1} \propto S_{C\text{-}D}^2$ for all C^2H_2 segment positions of the Pam_2-PtdCho bilayer at all temperatures (Fig. 1*a Inset*) (12). This would then imply that the temperature dependence of the acyl chain segment T_1 values of saturated lipid bilayers may be due to variations in the order parameter $S_{C\text{-}D}$ (= $S_{C\text{-}H}$) (12), contrary to previous interpretations in terms of an activation energy (9, 19, 26).

It is noteworthy that the relative contributions of the two terms of Eq. 2 may vary for different segmental positions of the same bilayer or for bilayers composed of different phospholipids. Thus, although the second T_{1s}^{-1} term of Eq. 2 may provide the dominant contribution to T_1^{-1} for the hydrocarbon chain segments of the Pam_2-PtdCho bilayer, the relative importance of the T_{1f}^{-1} and T_{1s}^{-1} terms for the glycerol backbone segments, head groups, acyl chain HC=CH groups of unsaturated bilayers, etc., is uncertain at present. For the case of local motions, the T_{1f}^{-1} contribution to T_1^{-1} may be relatively insensitive to the ordering (19, 20) in contrast to the T_{1s}^{-1} slow term (12). Recently, it has been shown by two laboratories that a minimum (35) can be observed in T_1 as a function of temperature in certain lipid sytems (36, 37). The observation of a T_1 minimum is important in that it allows an unambiguous determination of the effective correlation time for those motions that are most efficient near the resonance frequency in influencing the T_1 relaxation. However, the observation of a T_1 minimum does not rule out additional contributions from other types of motions, for both the amplitudes and correlation times are important. Thus, in the ^{31}P NMR studies of Seelig and coworkers (36), the relatively long correlation time of the phosphodiester moiety ($\approx 10^{-9}$ sec), which may participate in intermolecular electrostatic or hydrogen-bonding interactions (38), could lead to an increased contribution from local motions near the resonance frequency, thereby explaining the relatively short ^{31}P T_1 values and the presence of a T_1 minimum. Similar considerations hold for ^2H NMR studies of bilayers containing the bulky cholesterol molecule (37). In general, the possible effects of cholesterol and proteins (29, 39) on collective bilayer motions are poorly understood at present.

It also should be noted in Fig. 3*a* that the intercept at infinite frequency, obtained by plotting the ^{13}C T_1^{-1} rates of the Pam_2-PtdCho bilayer CH_2 groups vs. $\omega_C^{-1/2}$, yields a value of T_{1f}^{-1} that is similar or identical to the corresponding T_1^{-1} rates of the CH_2 groups of *n*-hexadecane (neglecting end effects). (Control studies of *n*-hexadecane and other *n*-alkanes show that T_1^{-1} does not exhibit a frequency dependence within experimental error; cf. Fig. 3*a*.) Thus, differences in the T_1^{-1} rates of saturated lipid bilayers such as Pam_2-PtdCho vs. the equivalent *n*-paraffinic liquids, which might be ascribed to differences in microviscosity if measurements are made at only a single resonance frequency (6, 22), most likely manifest the additional T_{1s}^{-1} contribution from relatively slow motions. As a result, the relaxation is more efficient in the saturated lipid bilayers, and the T_1 val-

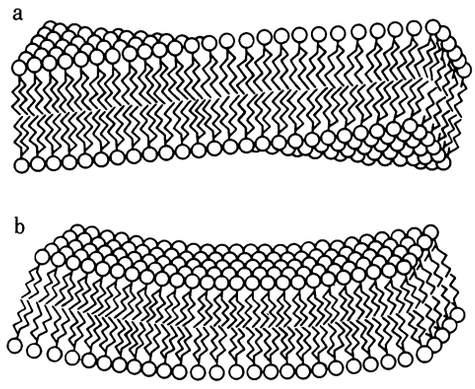

FIG. 4. Examples of the types of cooperative bilayer disturbances leading to the predicted $\omega_0^{-1/2}$ relaxation dependence, where $\omega_0 \equiv \omega_D, \omega_C$ is the nuclear resonance frequency. (*a*) Twist. (*b*) Splay.

ues are shorter than for the corresponding *n*-alkanes. This would in turn imply that the microviscosity values of the two systems are comparable, in contrast to earlier fluorescence depolarization results (40). It should be noted further that the value of $\tau_f \approx 10^{-11}$ sec obtained from the T_{1f}^{-1} contribution (12) is quite small relative to previous estimates (6, 19, 20) but appears consistent with recent stochastic dynamic simulations of model *n*-alkanes (24).

The various types of cooperative motions in lipid bilayers that might lead to the observed relaxation enhancement vs. *n*-alkanes are depicted schematically in Fig. 4. For clarity of presentation, relatively long wavelength modes are shown, which most likely would contribute to relaxation processes outside of the T_1 regime (i.e., at lower frequencies). By assuming a continuum description, however, similar shorter wavelength modes would influence the T_1 relaxation in the megahertz regime. The wavelengths of these modes would have to be substantially less than the diameter (≈300 Å) of the small, unilamellar vesicles to account for their similar T_1 values relative to multilamellar dispersions. It is interesting that certain of the longer wavelength modes may be frozen-out in the $L_\alpha \rightarrow P_{\beta'}$ phase transition of pure Pam_2-PtdCho dispersions (41). The relationship of any cooperative bilayer fluctuations to lateral self-diffusion of phospholipids in the liquid crystalline phase of lipid bilayers (15) appears to be uncertain at present—e.g., one might imagine that an upper bound to the lifetimes of the modes might be imposed by lateral diffusion or that diffusion of phospholipids through any relatively long-lived modes set up in the bilayer could affect the T_1 relaxation. For the case of the Pam_2-PtdCho vesicles used for the ^{13}C T_1 studies, however, lateral diffusion about the curved surface does not appear to greatly affect the relaxation because their T_1 values are similar to those of the corresponding multilamellar dispersions. Finally, it should be emphasized that the above paradigm, like any model, is subject to continued testing, refinement, and possible evolution.

Special thanks are due to the staff at the various NMR facilities where this work was performed—particularly William Hutton, Laura Lerner, Rudi Nunlist, Charles Schmidt, Charles Springer, and Dennis Torchia—for their patience and generous assistance. The deuterium T_1 data for the sonicated vesicles at 13.8 MHz were kindly provided by Jeffrey Browning. Expert technical assistance was rendered by Steven Dodd. We further wish to acknowledge critical discussions with Meyer Bloom, David Cafiso, James Davis, Ken Dill, Robert Griffin, Wayne Hubbell, Kenneth Jeffrey, Andrew McCammon, Harden McConnell, Joachim Seelig, Michael Sefcik, Attila Szabo, and Paul Ukleja. This work was supported by National Institutes of Health Grant R01 EY03754, the Cystic Fibrosis Foundation, and the Monsanto Corporation (M.F.B.); by National Science Foundation Chemical Instrumentation and National Institutes of Health Biomedical Research Grant Awards (University of Virginia); and by National Institutes of Health Grant RR00711 and National Science Foundation Grant GP23633 (Stanford Magnetic Resonance Laboratory). M.F.B. is an Alfred P. Sloan Research Fellow.

1. Penkett, S. A., Flook, A. G. & Chapman, D. (1968) *Chem. Phys. Lipids* **2,** 273–290.
2. Finer, E. G., Flook, A. G. & Hauser, H. (1971) *FEBS Lett.* **18,** 331–334.
3. Wennerström, H. & Lindblom, G. (1977) *Q. Rev. Biophys.* **10,** 67–96.
4. Seelig, J. (1977) *Q. Rev. Biophys.* **10,** 353–418.
5. Bloom, M., Burnell, E. E., MacKay, A. L., Nichol, C. P., Valic, M. I. & Weeks, G. (1978) *Biochemistry* **17,** 5750–5762.
6. Seelig, J. & Seelig, A. (1980) *Q. Rev. Biophys.* **13,** 19–61.
7. Griffin, R. G. (1981) *Methods Enzymol.* **72,** 108–174.
8. Levine, Y. K., Birdsall, N. J. M., Lee, A. G. & Metcalfe, J. C. (1972) *Biochemistry* **11,** 1416–1421.
9. Horwitz, A. F., Klein, M. P., Michaelson, D. M. & Kohler, S. J. (1973) *Ann. N.Y. Acad. Sci.* **222,** 468–488.
10. Chan, S. I., Sheetz, M. P., Seiter, C. H. A., Feigenson, G. W., Hsu, M.-C., Lau, A. & Yau, A. (1973) *Ann. N.Y. Acad. Sci.* **222,** 499–522.
11. Lee, A. G., Birdsall, N. J. M. & Metcalfe, J. C. (1974) in *Methods in Membrane Biology*, ed. Korn, E. D. (Plenum, New York), Vol. 2, pp. 1–156.
12. Brown, M. F. (1982) *J. Chem. Phys.* **77,** 1576–1599.
13. Ribeiro, A. A., King, R., Restivo, C. & Jardetzky, O. (1980) *J. Am. Chem. Soc.* **102,** 4040–4051.
14. Allison, S. A., Shibata, J. H., Wilcoxon, J. & Schurr, J. M. (1982) *Biopolymers* **21,** 729–762.
15. Edidin, M. (1974) *Annu. Rev. Biophys. Bioeng.* **3,** 179–201.
16. Op den Kamp, J. A. F. (1979) *Annu. Rev. Biochem.* **48,** 47–71.
17. Fung, B. K.-K. & Hubbell, W. L. (1978) *Biochemistry* **17,** 4403–4410.
18. Davis, J. H. (1979) *Biophys. J.* **27,** 339–358.
19. Brown, M. F., Seelig, J. & Haeberlen, U. (1979) *J. Chem. Phys.* **70,** 5045–5053.
20. Brown, M. F. (1979) *J. Magn. Reson.* **35,** 203–215.
21. Brainard, J. R. & Szabo, A. (1981) *Biochemistry* **20,** 4618–4628.
22. Lee, A. G., Birdsall, N. J. M., Metcalfe, J. C., Warren, G. B. & Roberts, G. C. K. (1976) *Proc. R. Soc. London, Ser. B* **193,** 253–274.
23. London, R. E. & Avitabile, J. (1977) *J. Am. Chem. Soc.* **99,** 7765–7776.
24. Levy, R. M., Karplus, M. & Wolynes, P. G. (1981) *J. Am. Chem. Soc.* **103,** 5998–6011.
25. Peterson, N. O. & Chan, S. I. (1977) *Biochemistry* **16,** 2657–2667.
26. Bocian, D. F. & Chan, S. I. (1978) *Annu. Rev. Phys. Chem.* **29,** 307–335.
27. Jeffrey, K. R., Wong, T. C., Burnell, E. E., Thompson, M. J., Higgs, T. P. & Chapman, N. R. (1979) *J. Magn. Reson.* **36,** 151–171.
28. Pace, R. J. & Chan, S. I. (1982) *J. Chem. Phys.* **76,** 4217–4247.
29. Brown, M. F., Deese, A. J. & Dratz, E. A. (1982) *Methods Enzymol.* **81,** 709–728.
30. Brown, M. F., Williams, G. D. & Ribeiro, A. A. (1982) *Biophys. J.* **37,** 13a (abstr.).
31. Sefcik, M. D., Schaefer, J., Stejskal, E. O., McKay, R. A., Ellena, J. F., Dodd, S. W. & Brown, M. F. (1983) *Biophys. J.* **41,** 282a (abstr.).
32. Brown, M. F. & Davis, J. H. (1981) *Chem. Phys. Lett.* **79,** 431–435.
33. de Gennes, P. G. (1974) *The Physics of Liquid Crystals* (Oxford University Press, London).
34. Farrar, T. C. & Becker, E. D. (1971) *Pulse and Fourier Transform NMR* (Academic, New York).
35. Carrington, A. & MacLachlan, A. D. (1967) *Introduction to Magnetic Resonance* (Harper & Row, New York).
36. Seelig, J., Tamm, L., Hymel, L. & Fleischer, S. (1981) *Biochemistry* **20,** 3922–3932.
37. Taylor, M. G., Akiyama, T., Saitô, H. & Smith, I. C. P. (1982) *Chem. Phys. Lipids* **31,** 359–379.
38. Seelig, J. (1978) *Biochim. Biophys. Acta* **505,** 105–140.
39. Deese, A. J., Dratz, E. A., Williams, G. D. & Brown, M. F. (1983) *Biophys. J.* **41,** 282a (abstr.).
40. Shinitzky, M. & Barenholtz, Y. (1978) *Biochim. Biophys. Acta* **515,** 367–394.
41. Falkovitz, M. S., Seul, M., Frisch, H. L. & McConnell, H. M. (1982) *Proc. Natl. Acad. Sci. USA* **79,** 3918–3921.